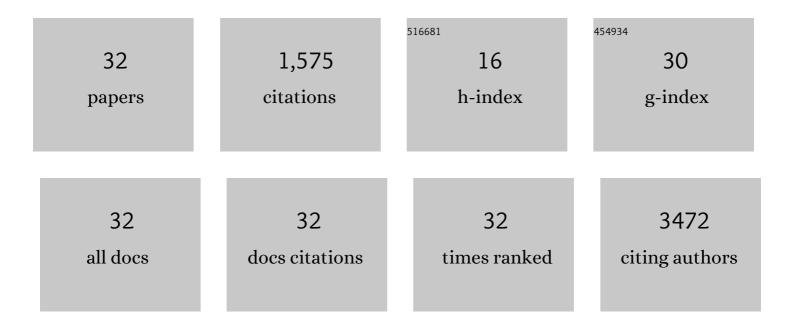
## Majid Ahmadi

List of Publications by Year in descending order

Source: https://exaly.com/author-pdf/6386011/publications.pdf Version: 2024-02-01



#	Article	IF	CITATIONS
1	Temperature-Dependent Raman Studies and Thermal Conductivity of Few-Layer MoS <sub>2</sub> . Journal of Physical Chemistry C, 2013, 117, 9042-9047.	3.1	602
2	Surface Energy Engineering for Tunable Wettability through Controlled Synthesis of MoS <sub>2</sub> . Nano Letters, 2014, 14, 4314-4321.	9.1	258
3	Reversible oxygen migration and phase transitions in hafnia-based ferroelectric devices. Science, 2021, 372, 630-635.	12.6	138
4	Gas–liquid segmented flow microwave-assisted synthesis of MOF-74(Ni) under moderate pressures. CrystEngComm, 2015, 17, 5502-5510.	2.6	68
5	Temperature dependent Raman scattering studies of three dimensional topological insulators Bi2Se3. Journal of Applied Physics, 2014, 115, .	2.5	56
6	Synthesis and characterization of tungstite (WO3·H2O) nanoleaves and nanoribbons. Acta Materialia, 2014, 69, 203-209.	7.9	55
7	Optical and Vibrational Studies of Partially Edge-Terminated Vertically Aligned Nanocrystalline MoS2 Thin Films. Journal of Physical Chemistry C, 2013, 117, 26262-26268.	3.1	51
8	Synthesis of tungsten oxide nanoparticles using a hydrothermal method at ambient pressure. Journal of Materials Research, 2014, 29, 1424-1430.	2.6	45
9	WO3 nano-ribbons: their phase transformation from tungstite (WO3·H2O) to tungsten oxide (WO3). Journal of Materials Science, 2014, 49, 5899-5909.	3.7	34
10	How Mn/Ni Ordering Controls Electrochemical Performance in High-Voltage Spinel LiNi <sub>0.44</sub> Mn <sub>1.56</sub> O <sub>4</sub> with Fixed Oxygen Content. ACS Applied Energy Materials, 2020, 3, 6001-6013.	5.1	33
11	Synthesis, characterization and understanding of the mechanisms of electroplating of nanocrystalline–amorphous nickel–tungsten alloys using in situ electrochemical impedance spectroscopy. Journal of Alloys and Compounds, 2013, 574, 196-205.	5.5	28
12	Large scale synthesis of single-crystal and polycrystalline boron nitride nanosheets. Journal of Materials Science, 2013, 48, 2543-2549.	3.7	25
13	A novel water-based epoxy coating using self-doped polyaniline–clay synthesized under supercritical CO2 condition for the protection of carbon steel against corrosion. Progress in Organic Coatings, 2015, 79, 90-97.	3.9	24
14	Single-step route to hierarchical flower-like carbon nanotube clusters decorated with ultrananocrystalline diamond. Carbon, 2013, 63, 253-262.	10.3	23
15	Single-step route to diamond-nanotube composite. Nanoscale Research Letters, 2012, 7, 535.	5.7	20
16	Synthesis of 2D Germanane (GeH): a New, Fast, and Facile Approach. Angewandte Chemie - International Edition, 2021, 60, 360-365.	13.8	17
17	Structural Dynamics and Tunability for Colloidal Tin Halide Perovskite Nanostructures. Advanced Materials, 2022, 34, e2201353.	21.0	16
18	<i>In situ</i> heating studies on temperature-induced phase transitions in epitaxial Hf0.5Zr0.5O2/La0.67Sr0.33MnO3 heterostructures. Applied Physics Letters, 2021, 118, .	3.3	15

Majid Ahmadi

#	Article	IF	CITATIONS
19	Unraveling dislocation mediated plasticity and strengthening in crack-resistant ZnAlMg coatings. International Journal of Plasticity, 2021, 144, 103041.	8.8	13
20	Infrared absorbance of vertically-aligned multi-walled CNT forest as a function of synthesis temperature and time. Materials Research Bulletin, 2020, 126, 110821.	5.2	11
21	Nickel oxide crystalline nano flakes: synthesis, characterization and their use as anode in lithium-ion batteries. Materials Research Express, 2014, 1, 025501.	1.6	8
22	Highly protective performance of water-based epoxy coating loaded with self-doped nanopolyaniline synthesized under supercritical CO2 condition. Progress in Organic Coatings, 2014, 77, 1977-1984.	3.9	8
23	Water-Soluble Derivatives of Octanuclear Iron-Oxido-Pyrazolato Complexes - an Experimental and Computational Study. European Journal of Inorganic Chemistry, 2012, 2012, 3704-3711.	2.0	7
24	Imaging atomic motion of light elements in 2D materials with 30 kV electron microscopy. Nanoscale, 2021, 13, 20683-20691.	5.6	5
25	Real-time imaging of atomic electrostatic potentials in 2D materials with 30 keV electrons. Microscopy and Microanalysis, 2021, 27, 1946-1947.	0.4	4
26	Doping of TiO2 nanopowders with vanadium for the reduction of its band gap reaching the visible light spectrum region. MRS Communications, 2014, 4, 73-76.	1.8	3
27	Growth of multi-layered graphene on molybdenum catalyst by solid phase reaction with amorphous carbon. 2D Materials, 2019, 6, 035012.	4.4	3
28	Locally Condensed Water as a Solution for In Situ Wet Corrosion Electron Microscopy. Microscopy and Microanalysis, 2020, 26, 211-219.	0.4	2
29	In-situ Electron Microscopy Observation of Initiation and Propagation of Wet H <sub>2</sub> S Corrosion on Steel. Microscopy and Microanalysis, 2021, 27, 242-245.	0.4	2
30	Monte Carlo Simulations of Electron Energy-Loss Spectra with the Addition of Fine Structure from Density Functional Theory Calculations. Microscopy and Microanalysis, 2016, 22, 219-229.	0.4	1
31	Shape-controlled synthesis of silver nanostructures for high-thermal conductivity nanofluids. Materials Research Society Symposia Proceedings, 2012, 1439, 33-38.	0.1	0
32	Direct observation of reversible oxygen migration and phase transitions in ferroelectric Hf0.5Zr0.5O2 thin-film devices. Microscopy and Microanalysis, 2021, 27, 956-959.	0.4	0